High-resolution vacuum-ultraviolet photoabsorption spectra of 1-butyne and 2-butyne

U. Jacovella, D. Holland, S. Boyé-Péronne, B. Gans, N. de Oliveira, D. Joyeux, L. Archer, R. Lucchese, H. Xu, S. Pratt

High-resolution vacuum-ultraviolet photoabsorption spectra of 1-butyne and 2-butyne

Cite as: J. Chem. Phys. **143**, 034304 (2015); https://doi.org/10.1063/1.4926541
Submitted: 15 March 2015 • Accepted: 23 June 2015 • Published Online: 16 July 2015

U. Jacovella, D. M. P. Holland, S. Boyé-Péronne, et al.

High-resolution vacuum-ultraviolet photoabsorption spectra of 1-butyne and 2-butyne

U. Jacovella,[1] D. M. P. Holland,[2] S. Boyé-Péronne,[3] B. Gans,[3] N. de Oliveira,[4] D. Joyeux,[4] L. E. Archer,[4] R. R. Lucchese,[5] H. Xu,[6,a)] and S. T. Pratt[6]
[1]*Laboratorium für Physikalische Chemie, ETH Zürich, 8093 Zürich, Switzerland*
[2]*STFC, Daresbury Laboratory, Daresbury, Warrington, Cheshire WA4 4AD, United Kingdom*
[3]*Institut des Sciences Moléculaires d'Orsay, UMR 8214, CNRS and Université Paris-Sud, F-91405 Orsay, France*
[4]*Synchrotron Soleil, L'Orme des Merisiers, F-91192 Gif-sur-Yvette, France*
[5]*Department of Chemistry, Texas A&M University, College Station, Texas 77843, USA*
[6]*Argonne National Laboratory, Argonne, Illinois 60439, USA*

(Received 15 March 2015; accepted 23 June 2015; published online 16 July 2015)

The absolute photoabsorption cross sections of 1- and 2-butyne have been recorded at high resolution by using the vacuum-ultraviolet Fourier-Transform spectrometer at the SOLEIL Synchrotron. Both spectra show more resolved structure than previously observed, especially in the case of 2-butyne. In this work, we assess the potential importance of Rydberg states with higher values of orbital angular momentum, l, than are typically observed in photoabsorption experiments from ground state molecules. We show how the character of the highest occupied molecular orbitals in 1- and 2-butyne suggests the potential importance of transitions to such high-l (l = 3 and 4) Rydberg states. Furthermore, we use theoretical calculations of the partial wave composition of the absorption cross section just above the ionization threshold and the principle of continuity of oscillator strength through an ionization threshold to support this conclusion. The new absolute photoabsorption cross sections are discussed in light of these arguments, and the results are consistent with the expectations. This type of argument should be valuable for assessing the potential importance of different Rydberg series when sufficiently accurate direct quantum chemical calculations are difficult, for example, in the $n \geq 5$ manifolds of excited states of larger molecules. [http://dx.doi.org/10.1063/1.4926541]

I. INTRODUCTION

The straight chain alkyne molecules are prototypical fuel species that can play an important role in hydrocarbon combustion and in the formation of soot. The Vacuum UltraViolet (VUV) photoabsorption and photoionization spectra of these species are of interest because they can provide insight into the electronic structure of these molecules, and because they highlight common features arising from the triple bond and its local environment within different molecules.[1–12] In addition, photoionization mass spectrometry is now commonly used to characterize species present in samples extracted from reacting environments, and absolute cross sections for these species allow their concentrations to be quantified.[13,14] The comparison of absolute photoabsorption and photoionization cross sections allows the determination of the quantum yields for ionization,[15,16] as well as an assessment of the importance of competing decay processes such as internal conversion, intersystem crossing, and predissociation.[17] An understanding of the systematic behavior of the photoabsorption and photoionization cross sections will also aid the development of general ideas for the estimation of absolute cross sections for related species,[18–20] including free radicals for which cross section determinations can be difficult.

The assignment of VUV photoabsorption spectra in medium- to large-sized molecules remains challenging for a number of reasons.[21–23] In particular, the symmetries of such molecules are often low, resulting in a large number of allowed transitions and increasing interactions among states. In addition, rotational structure is generally unresolved, and linewidths are often broadened by rapid radiationless transitions and predissociation, so that even the electronic structure is often only partially resolved, particularly above principal quantum number $n \sim 4$. While quantum chemical calculations are a great boon to the analysis of these spectra,[5,8] the current state-of-the-art is insufficient to make the assignments of the spectra based on energetics alone. As a result, phenomenological quantum defects, which tend to have characteristic values for each value of orbital angular momentum, l, and assumptions about which series are generally strong (the penetrating s, p, and d series) and weak (the non-penetrating f, g, ... series) are used to guide the analysis.[21–23] However, in some larger molecules, the nodal structure of the highest occupied molecular orbital (HOMO) and more strongly bound orbitals can become more complex, taking on character associated with higher l states than generally expected. In such situations, the standard assumptions (quantum defects

a)Present address: Brookhaven National Laboratory, Department of Chemistry, Upton, New York 11973, USA.

for $l \geq 3 \sim 0$; transitions to states with $l \geq 3$ are weak) are likely to break down.

As discussed below, the *n*-alkynes represent one group of molecules for which this breakdown may occur. In the absence of quantitatively accurate electronic structure calculations, additional insight is required to complement the traditional approach to analysis. In the present study, we make use of two ideas. First, we use the nodal structure of the HOMOs and (HOMO-1)s to make an assessment of which Rydberg series are likely to be strong. Second, we use calculations of the photoabsorption cross section just above the ionization threshold to determine which partial waves (l values) are strong in the continuum and then use the continuity of oscillator strength[24,25] through the ionization threshold to predict which nl Rydberg series will be strong just below threshold. While such calculations do not predict the positions of the Rydberg states, they do provide a strong indication of which series can be expected in the spectrum.

As an example, the low-resolution photoionization cross sections for acetylene, propyne, and 1-butyne show similar behaviors,[11,12,26] with a relatively rapid rise at threshold leading to a plateau that extends for 2–3 eV above threshold. In contrast, the photoionization cross section for 2-butyne shows very different behavior, with a very intense broad resonance just above threshold that has a peak cross section ~3 times greater than the values for the three other alkynes.[11,12,26] Understanding the source of this high cross section is important, and in this case, the intense feature has been found to arise from a shape resonance in the continuum,[9] corresponding to a resonance in the $l = 4\ g\pi_g$ electron continuum. Because this resonance is so intense and broad, its influence is expected to extend below the ionization threshold in 2-butyne, leading to an expected increase in the intensity of the bound $l = 4\ g\pi_g$ Rydberg series in this molecule. Symmetry arguments can explain why this resonance is not important for acetylene, propyne, and 1-butyne, and not likely to be important for the propargyl radical.[9]

The HOMOs of the four smallest closed-shell alkynes correspond to degenerate (or nearly degenerate) π orbitals centered on the C≡C triple bond. In acetylene, the HOMO looks like a stretched $p\pi_u$ orbital,[27] and the ground state of the cation is a linear $^2\Pi$ state that is split by Renner-Teller interactions upon excitation of two nontotally symmetric vibrations. In propyne[27] and 1-butyne,[9] the HOMOs are very similar and look like asymmetric $d\pi_g$ orbitals with the principal pair of lobes on the C≡C triple bond and a second out-of-phase pair of lobes on the adjacent CH_3 or CH_2. As a result, considerable similarities are expected in the Rydberg state structure of the two molecules. The asymmetry of the HOMOs of propyne and 1-butyne indicates that a single-center expansion would contain substantial atomic *n*p and *n*d character. Indeed, a single-center expansion of the propyne HOMO about the central C atom gives 54% p and 28% d character.[7] The substantial d character in the HOMO of propyne suggests that transitions to *n*f Rydberg series may be important, and we have recently presented evidence for such transitions in the photoabsorption spectrum.[7] Given the similarity of the propyne and 1-butyne HOMOs,[9] such *n*f Rydberg series are also expected to have

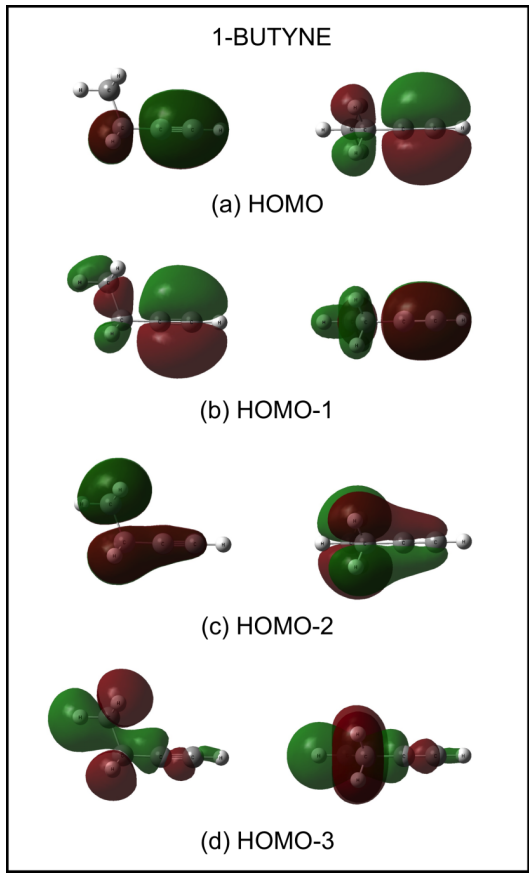

FIG. 1. (a) The highest occupied molecular orbital (HOMO) for the ground state of 1-butyne; (b) the HOMO-1; (c) the HOMO-2; (d) the HOMO-3.

significant intensity in the photoabsorption spectrum of 1-butyne.

The HOMO and several other orbitals of 1-butyne and 2-butyne are shown in Figures 1 and 2, respectively. The molecular geometries were optimized by using the second order Møller-Plesset (MP2) method, and the orbitals correspond to Hartree-Fock orbitals computed with a 6-311G(2df,p) basis set by using the Gaussian 09 suite of programs.[28] The HOMO of the 2-butyne is far more symmetric than the HOMO of propyne and 1-butyne and has the appearance of a stretched $f\pi_u$ orbital. The single-center expansion of this orbital is expected to have considerable p ($p\pi_u$) and f ($f\pi_u$) character. The significant f character in the HOMO is an important factor that contributes to the large intensity of the $g\pi_g^*$ shape resonance above threshold,[9] as well as to any oscillator strength in the $g\pi_g$ Rydberg series below threshold.

The room-temperature photoabsorption spectrum of 1-butyne has been reported at moderate resolution (~40–70 cm^{-1} in the region of interest) by Nakayama and Watanabe together with the values of the absorption coefficients.[2] They assigned three Rydberg series by analogy with the spectrum of propyne; for some Rydberg states, they also tentatively assigned progressions involving the ν_3 C≡C stretching vibration and the ν_2 C—C stretching vibration. In general, the authors found the features to be quite broad, adding to the difficulty of making definitive assignments.[2] The room-temperature photoabsorption spectrum of 2-butyne has been reported more recently by Palmer and Walker.[8] This spectrum shows

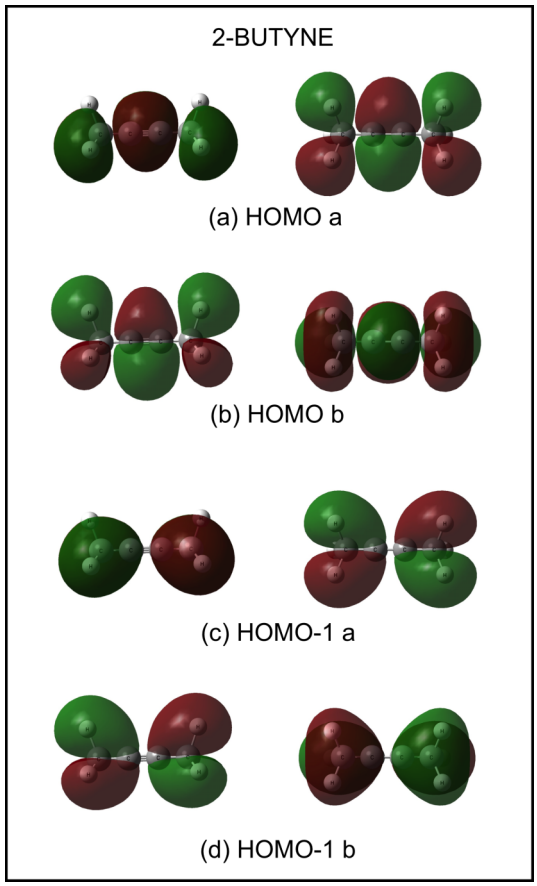

FIG. 2. (a) and (b) show the two components of the degenerate highest occupied molecular orbital (HOMO) for the ground state of 2-butyne; (c) and (d) show the two components of the degenerate HOMO-1.

considerably more sharp structure than the earlier spectrum of 1-butyne. Palmer and Walker[8] also performed high-level theoretical calculations on the valence states and *n*s, *n*p, and *n*d Rydberg states converging to the ground electronic state of the cation. They were able to assign a number of Rydberg series, along with a significant amount of associated vibrational structure associated with the ν_3 C≡C stretching vibration.[8] [Note that the previous researchers have labelled the C≡C stretching vibration as ν_3 in 1-butyne[2] and ν_2 in 2-butyne.[8] Although this scheme may be somewhat confusing, we have chosen to follow these precedents.] No evidence was presented for *n*f or higher *l* Rydberg series in 2-butyne. In light of the discussion above, a re-examination of the photoabsorption spectra of 1- and 2-butyne is in order.

In the present paper, we report new high-resolution photoabsorption cross sections for 1- and 2-butyne recorded by using the Vacuum-UltraViolet Fourier Transform Spectrometer (VUV-FTS) on the DESIRS (Dichroïsme Et Spectroscopie par Interaction avec le Rayonnement Synchrotron) beamline at the SOLEIL Synchrotron.[29,30] The resolution is substantially improved over the previously reported spectra, and the absolute cross sections at room temperature are determined. Because of the nature of the spectrometer, the band positions are also determined with high precision. The spectrum of 1-butyne is somewhat better resolved than the earlier spectrum[2] and provides much better definition of the vibrational progressions in the ν_2 and ν_3 vibrational modes. However, no new Rydberg series are identified. The spectrum of 2-butyne shows considerably more structure than in the previous study,[8] and Rydberg series can be extended to somewhat higher principal quantum number. Evidence for higher *l* Rydberg series is discussed.

In what follows, we first discuss the experimental and theoretical approaches. Next, we present the experimental photoabsorption data for 1- and 2-butyne and discuss them in the context of previous experiments. We then consider an alternative assignment for some of the features in the 2-butyne spectrum and provide a theoretical justification for this assignment. The discussion of the spectra is concluded with some thoughts on the generality of the observations and the implications for larger alkynes.

II. EXPERIMENT

The VUV-FTS has been described in detail previously,[29,30] and we limit the description to the specific details of the present experiment. The spectra of 1- and 2-butyne were recorded by using two different sample cells: a windowed cell for calibrating the absolute photoabsorption cross sections and a flowing cell for recording high-resolution, room-temperature spectra. The determination of absolute photoabsorption cross sections in the flowing cell requires a systematic calibration procedure using measurements from the windowed cell under the same conditions. This procedure has been described previously.[29–31] The resulting calibration curve is used over the full VUV range including the windowless part of the spectrum. Experimental uncertainties in the cross section determinations in the flowing cell are estimated to be about ±10%, mainly due to the column density calibration curve. A detailed discussion of the FTS calibration process and the potential sources of error in cross sections will be presented in a forthcoming publication.[31] 1-butyne (ABCR GmbH & Co., 98% purity) is a gas at room temperature and was used directly from the cylinder. 2-butyne (ABCR GmbH & Co., 98% purity) is a high-vapor pressure liquid at room temperature, and the gas above the liquid was used.

Individual sections of the full spectrum were recorded at one of the thirteen undulator settings used to cover the energy region between 46 000 cm^{-1} and 90 000 cm^{-1}. Each spectrum used the full bandwidth of the undulator after the synchrotron light had passed through a harmonic-removing gas filter. The full spectrum was then obtained by splicing together the individual spectra and calibrated by using impurity lines in the gas filter. [The observed impurity lines correspond to Xe: 68 045.15 cm^{-1}, 77 185.04 cm^{-1}, and 83 889.97 cm^{-1}; Kr: 80 916.76 cm^{-1} and 85 846.70 cm^{-1}; O: 76 794.97 cm^{-1}; and H: 82 259.15 cm^{-1}.[32]] As in any Fourier-Transform spectrometer, the spectral resolution is determined by the maximum optical pathlength difference in the interferometer. The room-temperature spectra reported here were recorded at a resolution of 0.86 cm^{-1}, but the spectra for 2-butyne were processed to give better signal-to-noise ratio resulting in an effective resolution of 3.4 cm^{-1} with no apparent loss of information. The resolution was confirmed by the measured linewidths of the atomic impurity transitions.[32]

III. RESULTS AND DISCUSSION

A. 1-butyne

The 1-butyne molecule is a nonlinear asymmetric top with C_s symmetry. Figure 3 shows the photoabsorption spectrum of 1-butyne obtained in the flowing cell. In general, the agreement with the spectrum of Nakayama and Watanabe is excellent.[2] The cross section values on some of the most intense peaks are ~8% greater than the earlier values, which most likely results from the higher resolution in the present spectrum. However, this discrepancy is also within the expected error (5%-10%) of the present spectrum. As discussed below, the higher resolution also reveals some vibrational structure that is not visible in the earlier spectrum, but for the most part, the spectra are similar. The band positions and assignments are given in Table I.

Carlier *et al.*[33] have used photoelectron spectroscopy to determine the first ionization energy of 1-butyne, yielding a value of $82\,090 \pm 40$ cm^{-1}. This value is in agreement with that determined by Nakayama and Watanabe[2] from their photoionization threshold and their analysis of Rydberg series (82 100 cm^{-1}). Nakayama and Watanabe identified three Rydberg series of 1-butyne, which they labeled R, R′, and R″ in analogy with their analysis of propyne.[2] These series are

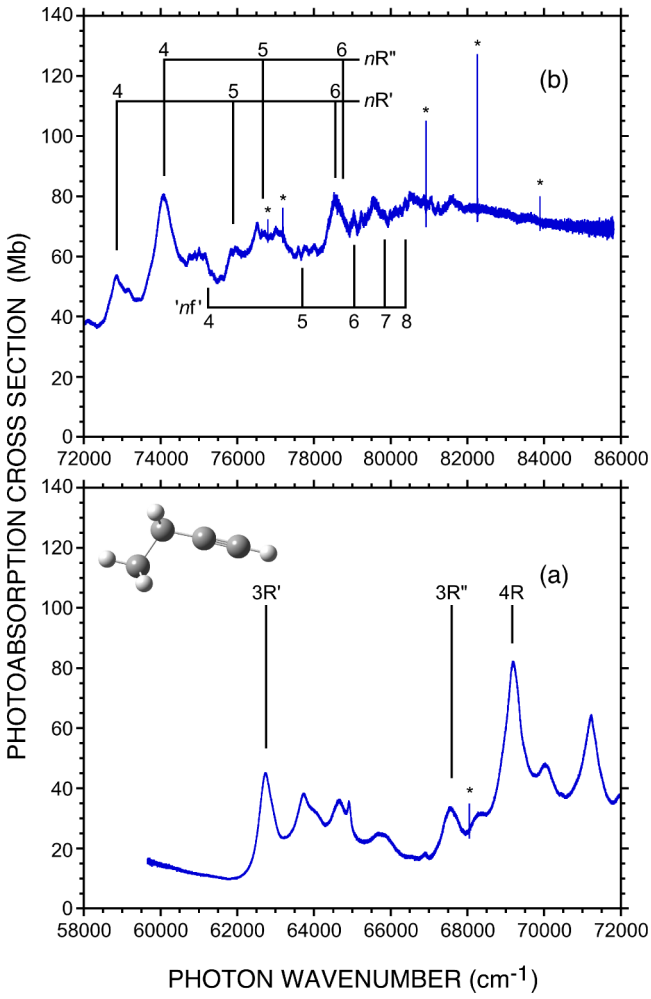

FIG. 3. The room-temperature absolute photoabsorption cross section of 1-butyne. The sharp lines marked by asterisks correspond to absorption transitions in atomic impurities (see text in Sec. II).

TABLE I. Band positions for 1-butyne.

Band position (cm^{-1})	Assignment	n^* (82 090 cm^{-1})[a]	Peak absorption cross section (Mb)
62 733.70	3R′	2.3810	44.8
63 727.60	3R′ + ν_2	2.4446	38.1
64 031.90		2.4651	31.9
64 653.40	3R′ + 2ν_2	2.5087	35.6
64 913.50	3R′ + ν_3	2.5276	35.3
65 762.40	3R′ + 3ν_2	2.5925	24.7
66 900.60	3R′ + 2ν_3	2.6878	18.3
67 547.70	3R″	2.7470	33.1
68 281.00		2.8190	31.2
68 961.10		2.8911	56.3
69 190.20	4R	2.9166	81.5
69 479.40		2.9499	53.4
70 043.60	4R + ν_2	3.0182	47.7
70 458.10		3.0715	37.9
71 222.90	4R + ν_3	3.1777	63.9
71 975.50		3.2938	37.5
72 106.30	4R + ν_2 + ν_3	3.3153	38.6
72 253.60		3.3401	37.5
72 695.30		3.4177	45.9
72 847.00	4R′	3.4456	53.1
72 978.70		3.4704	50.3
73 162.00	4R + 2ν_3	3.5059	48.8
73 767.70		3.6312	57.5
74 071.20	4R″	3.6993	80.0
74 592.20		3.8257	58.8
74 755.80		3.8681	60.3
74 892.80		3.9047	60.6
75 003.30		3.9351	62.2
75 168.90		3.9819	60.6
75 356.00		4.0368	54.1
75 573.60		4.1037	52.8
75 832.70		4.1878	61.6
75 959.50		4.2308	62.5
76 517.60		4.4377	70.6
76 652.20		4.4922	67.8
76 708.00		4.5155	68.1
76 856.90		4.5793	67.2
77 007.20		4.6465	69.1
77 160.50		4.7182	67.5
77 393.70		4.8339	62.2
77 592.00		4.9393	62.8
77 751.90		5.0295	63.1
77 804.90		5.0605	62.8
78 011.00		5.1868	63.4
78 389.00		5.4452	71.3
78 523.50		5.5469	79.4
78 967.30		5.9280	70.9
79 036.00		5.9943	73.8
79 230.70		6.1951	73.8
79 316.60		6.2903	73.1
79 408.20		6.3968	74.7
79 538.00		6.5574	78.8
79 591.00		6.6266	78.1
79 820.40		6.9534	74.1
79 982.40		7.2157	74.7
80 131.90		7.4861	75.3
80 246.40		7.7151	75.8
80 372.40		7.9931	78.3
80 495.50		8.2959	80.0

TABLE I. (*Continued.*)

Band position (cm^{-1})	Assignment	n^* (82 090 cm^{-1})[a]	Peak absorption cross section (Mb)
80 558.50		8.4648	80.4
80 866.70		9.4713	79.0
81 052.80		10.2859	78.4
81 236.60		11.3396	77.0
81 551.50		14.2752	79.1
81 612.10		15.1533	78.9
81 824.20		20.3189	77.0

[a]The effective principal quantum numbers were calculated by using Equation (1), the ionization energy for 1-butyne (82 090 cm^{-1}) and the Rydberg constant for 1-butyne (109 736.2 cm^{-1}).

given by

$$E_n = E_{ie} - R/(n-\delta)^2, \quad (1)$$

where E_{ie} is the ionization energy, R is the Rydberg constant for 1-butyne (109 736.2 cm^{-1}), n is the principal quantum number, and δ is the quantum defect. Nakayama and Watanabe[2] found $\delta = -0.08$ with $n = 4,5,\ldots$ for the R series, $\delta = +0.55$ with $n = 3,4,\ldots$ for the R′ series, and $\delta = +0.33$ with $n = 3,4,\ldots$ for the R″ series. These states are indicated in Figure 3. However, the present labels are limited to values $n < 6$, as no obvious assignments can be made above this. As seen in Figure 3(b), the spectrum above ~75 000 cm^{-1} ($n \sim 5$) is quite irregular and it is difficult to find any series with a constant quantum defect. Unlike the spectrum of propyne,[7] plotting the spectrum of 1-butyne against the effective principal quantum number is of little help. The lack of identifiable regular structure in the Rydberg series of 1-butyne may be a result of more extensive vibrational structure than in 2-butyne or smaller alkynes.

Figure 3 also shows the predicted positions for a series of *n*f Rydberg states converging to the ground electronic state of the ion and calculated by using Equation (1) with $\delta = 0.0$. Although weak structure is observed near each of these positions, no regular series of bands can be unambiguously identified. This observation suggests that either transitions to the *n*f states of 1-butyne are weak or irregular or that the *n*f series have quantum defects somewhat different from zero. The present spectra were recorded at room-temperature, and it is noteworthy that the *n*f series of propyne only became obvious in the jet-cooled sample.

In the photoelectron spectrum of 1-butyne, Carlier *et al.*[33] identified two progressions, with vibrational wavenumbers of 1980 ± 50 cm^{-1} and 890 ± 50 cm^{-1}, which they assigned to the ν_3 C≡C stretch and the ν_2 C—C stretch of the bond adjacent to the C≡C bond, respectively. Figure 4 shows an expanded portion of the 1-butyne absorption spectrum displaying evidence for similar vibrational progressions in the 3R′ band. The corresponding fundamental wavenumbers for the 3R′ state are 2180 cm^{-1} and 994 cm^{-1} for ν_3 and ν_2, respectively. Nakayama and Watanabe[2] previously identified the ν_2 progression, but the new spectrum also clearly shows two members of the progression in ν_3.

Figure 5 shows an expanded portion of the 1-butyne spectrum detailing the vibrational structure of the 4R band.

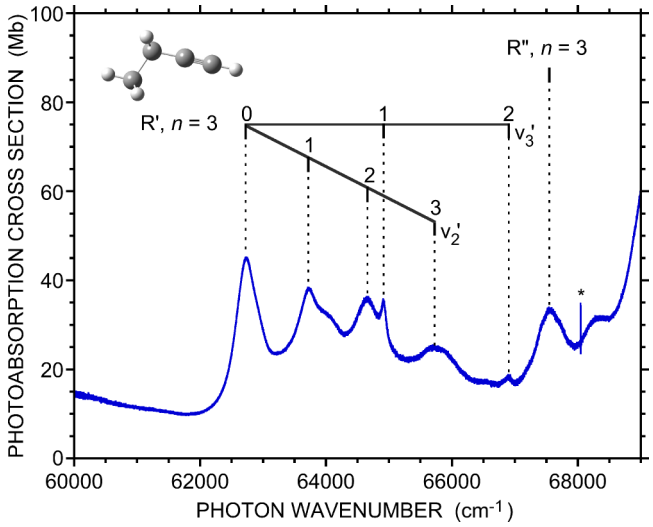

FIG. 4. An expanded portion of the room-temperature absolute photoabsorption cross section of 1-butyne in the region of $n^* = 3$. The sharp line marked by an asterisk corresponds to an absorption transition in an atomic impurity (see text in Sec. II).

This structure is not nearly as obvious or extended as that for the 3R′ band. Two progressions can be tentatively assigned to the ν_3 and ν_2 vibrations, with fundamental wavenumbers of 2033 cm^{-1} and 853 cm^{-1}, respectively.

Figure 6 shows the photoabsorption spectrum of 1-butyne in the region of the ionization threshold, along with the photoionization cross section from Wang *et al.*[12] As noted by Nakayama and Watanabe,[2] the quantum yield for ionization is much less than one, and the slow rise of the photoionization cross section just above threshold relative to the flat photoabsorption cross section suggests that the photoionization process is significantly less vertical than for similar species like propyne. This slow rise indicates a change in structure upon ionization of 1-butyne. This observation indicates that there is significant intensity in the Rydberg series converging to vibrationally excited states of the cation. However, the flat photoabsorption spectrum in this region

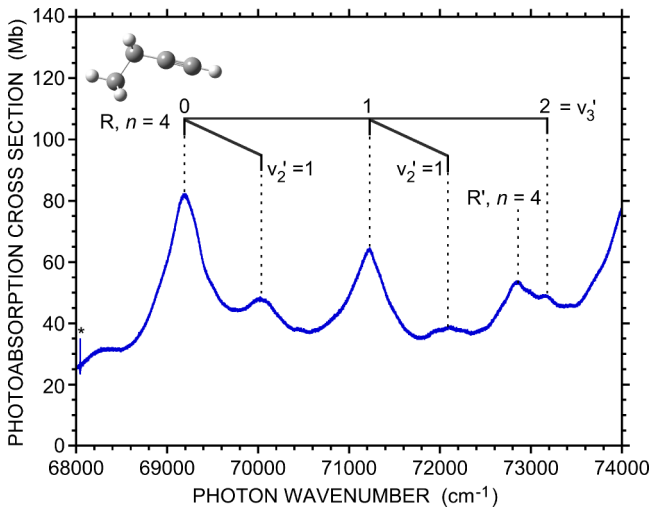

FIG. 5. An expanded portion of the room-temperature absolute photoabsorption cross section of 1-butyne in the region of $n^* = 4$.

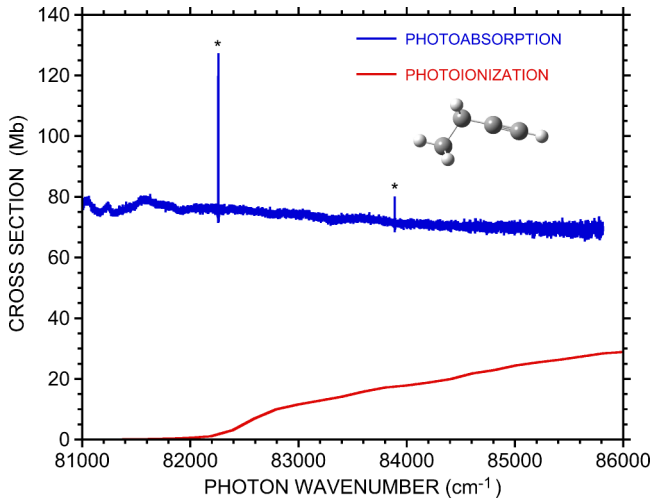

FIG. 6. The room-temperature absolute photoabsorption and photoionization cross sections of 1-butyne in the region of the first ionization threshold. The photoionization data are from Ref. 11. The sharp lines marked by asterisks correspond to absorption transitions in atomic impurities (see text in Sec. II).

suggests that these series must be broadened to the extent that they are not resolved. These observations indicate that the quantum yield for ionization of these vibrationally excited Rydberg series must also be significantly less than one. In other words, above the first ionization threshold, these Rydberg series still appear to be strongly predissociated.

B. 2-butyne

The electronic ground state of the 2-butyne molecule has a linear C—C≡C—C backbone,[9] while that of the ground state cation is nearly linear. The minimum energy in the neutral corresponds to the eclipsed geometry of the two CH_3 groups (D_{3h} symmetry), but the barrier to internal rotation is minimal (5.98 ± 0.03 cm^{-1}).[34] Calculations indicate that the geometry of the ground state cation (and presumably the geometries of the Rydberg series converging to the ground state cation) is neither D_{3h} nor D_{3d}, but rather C_{2h} or C_{2v}, because Jahn-Teller interactions slightly distort the linear carbon backbone.[9] As in the neutral ground state, the methyl groups undergo essentially free rotation. As noted by Palmer and Walker,[8] to first order, the vibrational progressions in the Rydberg states converging to the ground state of the ion should mirror those observed in the photoelectron spectrum for that state. This photoelectron spectrum is dominated by the origin band,[9,33,35] and the strongest observed progression is in the ν_2^+, C≡C stretching vibration ($\tilde{\nu}_2^+ = 2170 \pm 30$ cm^{-1}).[9] Progressions in the photoelectron spectrum have also been identified for the ν_4^+, C—C stretching vibration ($\tilde{\nu}_4^+ = 725 \pm 25$ cm^{-1}).[9] Theoretical vibrational wavenumbers for all of the vibrational modes for the neutral and ionic ground states of 2-butyne are given in Table 1 of Ref. 9, and we use the notation for the modes described therein. For the discussion below, we note that the theoretical vibrational wavenumber of the cation's ν_{11b}^+ mode, CH_3 rock, is 424 cm^{-1}, and the two components of the $\nu_{16a,b}^+$ C—C—C deformation are 418 cm^{-1} and 358 cm^{-1}. The ν_{11b}^+ is expected to be an active mode of the linear Jahn-Teller effect and is more likely to be observed than the $\nu_{16a,b}^+$ mode.[36] The adiabatic ionization energy of 2-butyne has recently been determined to be $77\,115.1 \pm 2.0$ cm^{-1}.[36] The ground state cation also has a small spin-orbit splitting that is not resolved in the present spectra; because this splitting is small, we use the center of gravity of the spin orbit states (77 120 cm^{-1}) in the calculation of the n^* values given in Table II.

Figure 7 shows an overview room-temperature absorption spectrum of 2-butyne. The line positions and assignments are given in Table II. Throughout the spectrum, the energy scale appears to differ from that of Ref. 8 by approximately 0.1%. In the discussion and figures presented below, the assignments of Ref. 8 have been shifted accordingly to match with the positions of the features in the present spectrum. Between approximately 50 000 cm^{-1} and 75 000 cm^{-1}, the absolute photoabsorption cross sections are in reasonably good agreement with the previous values of Palmer and Walker.[8] As seen in Figure 8, at higher energy, the present measurements are somewhat lower than those of Palmer and Walker,[8] particularly at the large resonance feature at ~80 000 cm^{-1} in the continuum, where the present values are approximately 35% below the earlier measurements. Because the present measurements expose the sample to the full undulator envelope at all times, there is a significantly greater possibility for depletion of the effective sample pressure by photodissociation of the sample during the measurement. This issue is not likely to be important in the earlier measurements, where the sample was exposed to a much weaker, monochromatized photon beam. While this difference in sample exposures could explain the observed differences in the cross sections, repeated measurements with shorter exposure times did not result in substantially different cross sections. Thus, the source of this discrepancy cannot be identified at this time. Figure 8 also shows the total photoionization cross section for 2-butyne from Wang *et al.*[12] At ~10 eV, this photoionization cross section[12] has nearly the same value as the present photoabsorption cross section. This observation would indicate a quantum yield for ionization of 100%, which is somewhat unusual so close to the ionization threshold.

The first ultraviolet absorption bands in 2-butyne are observed at ~50 000 cm^{-1} and correspond to weak, broad bands. Below 63 000 cm^{-1} (Figure 7(a)), the absorption bands have been discussed by Palmer and Walker,[8] and by Hamai and Hirayama,[10] and assigned to 3s and 3p Rydberg states and their associated vibrational structure. The first intense group of bands is observed between 63 000 cm^{-1} and 69 000 cm^{-1}, and Figure 9 shows an expanded view of this region of the spectrum. The assignment of the three principal Rydberg states in this figure follows the assignments of Palmer and Walker,[8] who based their assignment on quantum chemical calculations. Palmer and Walker[8] assigned the ν_2' = 0-2 bands of all three states ($3d_{y^2}$, $3d_{yz}$, and $3d_{xy,x^2-y^2}$, where the latter indicates two overlapped electronic states). Palmer and Walker[8] also assigned the bands at 63 560 cm^{-1} and 63 903 cm^{-1} to the ν_2' levels of the $3p_z$ and $3p_x$ Rydberg states, respectively. However, because the same pattern of two bands is observed in the same location relative to the $3d_{y^2}$, ν_2' = 0, 1, and 2 states, we have reassigned these bands to the ν_2' = 0–2, ν_{11b}' = 1, and ν_2' = 0–2, ν_4' = 1 bands. The ν_{11b} vibration corresponds to the b_1 component of the CH_3 rock, while the ν_4 vibration

TABLE II. Band positions for 2-butyne.

Band position (cm^{-1})	Assignment (Ref. 8)[a]	Assignment (present work)	n^* (77 120 cm^{-1})[b]	Peak absorption cross section (Mb)
51 263.80	3s	3s	2.0601	3.0
53 546.00	$3s+\nu_2$	$3s+\nu_2$	2.1575	3.2
54 895.70			2.2221	2.9
56 024.50			2.2808	2.9
57 030.70			2.3372	3.1
58 576.70			2.4327	4.3
59 435.60	$3p_z$	$3p_z$	2.4910	6.5
60 220.90			2.5483	6.2
60 576.70	$3p_x$	$3p_x$	2.5755	6.9
61 386.50			2.6410	6.4
61 631.90	$3p_z+\nu_2$	$3p_z+\nu_2$	2.6618	6.6
62 098.20			2.7028	7.1
62 269.90	$3p_x+\nu_2$	$3p_x+\nu_2$	2.7184	7.5
62 834.40			2.7716	7.9
63 182.00	$3d_{y^2}$	3d/4s	2.8059	92.7
63 570.50	$3p_z+2\nu_2$		2.8459	15.1
63 893.70	$3p_x+2\nu_2$		2.8804	22.9
64 257.30		3d/4s	2.9209	85.9
64 357.50	$3d_{yz}$		2.9323	76.6
64 575.10		3d/4s	2.9576	63.5
64 626.60	$3d_{xz,x^2-y^2}$		2.9637	63.5
64 812.70			2.9860	39.3
64 932.50			3.0007	26.3
65 317.80	$3d_{y^2}+\nu_2$	$3d/4s+\nu_2$	3.0493	47.9
65 712.90			3.1016	19.3
65 982.00			3.1389	23.4
66 404.90	$3d_{yz}+\nu_2$	$3d/4s+\nu_2$	3.2002	41.9
66 721.90	$3d_{xz,x^2-y^2}+\nu_2$	$3d/4s+\nu_2$	3.2486	31.5
66 957.10			3.2860	20.8
67 084.90			3.3069	17.2
67 422.30	$3d_{y^2}+2\nu_2$	$3d/4s+2\nu_2$	3.3639	18.5
67 810.80			3.4334	11.2
68 103.30			3.4886	12.2
68 456.00			3.5589	14.6
68 568.50	$3d_{yz}+2\nu_2$	$3d/4s+2\nu_2$	3.5822	15.3
68 865.00			3.6460	14.7
69 084.90	$3d_{xz,x^2-y^2}+2\nu_2$	$3d/4s+2\nu_2$	3.6956	18.4
69 492.00		4d/5s	3.7929	37.9
69 627.00	$4d_{y^2}$	4d/5s	3.8269	48.0
69 835.60	$4d_{yz}$	4d/5s	3.8813	53.3
69 926.40			3.9057	33.6
70 024.50			3.9326	26.1
70 240.50			3.9939	24.4
70 419.00	$4d_{xz,x^2-y^2}$	4fδ	4.0468	70.0
70 529.20			4.0804	20.4
70 906.80			4.2026	20.6
71 144.00			4.2852	20.0
71 289.20			4.3382	20.4
71 360.70			4.3651	20.2
71 567.00	$4d_{y^2}+\nu_2$		4.4454	27.9
71 749.30			4.5202	29.0
71 913.50			4.5910	45.6
71 983.40		5d/6s	4.6221	52.2
72 064.40			4.6590	47.3
72 196.90		5d/6s	4.7213	48.1
72 569.30	$5d_{yz}$, $4d_{xz,x^2-y^2}+\nu_2$	5fδ	4.9106	59.4
72 855.20	5d	5gπ	5.0726	44.8
73 106.30			5.2288	21.2
73 301.00			5.3605	27.1

TABLE II. (*Continued.*)

Band position (cm^{-1})	Assignment (Ref. 8)[a]	Assignment (present work)	n^* (77 120 cm^{-1})[b]	Peak absorption cross section (Mb)
73 479.40			5.4902	39.6
73 619.50			5.5990	49.8
73 678.90		6d/7s	5.6471	53.5
73 815.90		6d/7s	5.7630	47.1
73 979.80			5.9115	51.0
74 008.40	6d	6fδ	5.9386	55.2
74 156.40		6gπ	6.0851	44.8
74 389.40			6.3394	38.1
74 515.30			6.4908	43.8
74 585.50		7d/8s	6.5801	48.3
74 707.40		7d/8s	6.7443	61.0
74 839.90	7d	7fδ	6.9374	59.0
74 964.20		7gπ	7.1346	44.6
75 223.50		8d/9s	7.6068	49.6
75 383.80	8d	8fδ	7.9502	53.8
75 452.60		8gπ	8.1125	43.1
75 659.90		9d/10s	8.6693	56.5
75 759.70		9fδ	8.9817	60.8
75 929.90		10d/11s	9.6025	60.0
75 977.30			9.7996	62.1
76 160.10	$6d + \nu_2$	11d/12s	10.692	61.2
76 195.70			10.896	61.5
76 230.10			11.105	60.6
76 320.00		12d/13s	11.712	62.3
76 446.00		13d/14s	12.760	53.3
76 480.40			13.099	52.9
76 645.60			15.209	57.8
76 734.00			16.861	61.9
76 838.70			19.751	66.7
76 979.40	$7d + \nu_2$		27.937	67.1
77 097.10			69.227	64.8
77 393.10				66.9
77 526.00				70.6
77 605.70				66.5
77 809.00				70.8
77 905.10				72.7
78 117.80				75.8
78 344.00				75.0
78 469.90				76.9
78 598.80				75.0
78 793.50				76.6
79 042.90				79.7
79 227.00				80.7
79 620.70				83.2
79 953.00				84.5
80 218.80				86.3
80 462.20				87.2
80 613.50				88.1

[a]The peaks are somewhat more resolved in the present spectrum than in Ref. 8, and the resulting line positions are somewhat different. As a result, we have associated the assignments from Ref. 8 with the nearest peaks observed in the present spectrum.
[b]The effective principal quantum numbers were calculated by using Equation (1), the 2-butyne ionization energy[36] to the center of gravity of the two spin-orbit states of the ion (77 120 cm^{-1}), and the Rydberg constant for 2-butyne (109 736.2 cm^{-1}).

corresponds to an a_1 symmetry C—C stretch in the cation. The observed spacings are consistent with the calculated ionic frequencies for the ν_4^+ and ν_{11b}^+ modes. The intensities and progressions observed in Figure 9 are consistent with the photoelectron spectra presented previously,[9] which show a dominant origin band, a strong progression in ν_2^+, and a weaker progression in ν_4^+. The intensity of the $\nu_2^+ = 1$ photoelectron band is also approximately half that of the origin band.

Figure 10 shows the same spectral region as Figure 9 but is extended to include the regions corresponding to the n = 4–6 Rydberg states. Figure 10(a) shows the earlier assignments of Palmer and Walker,[8] which were based on their quantum

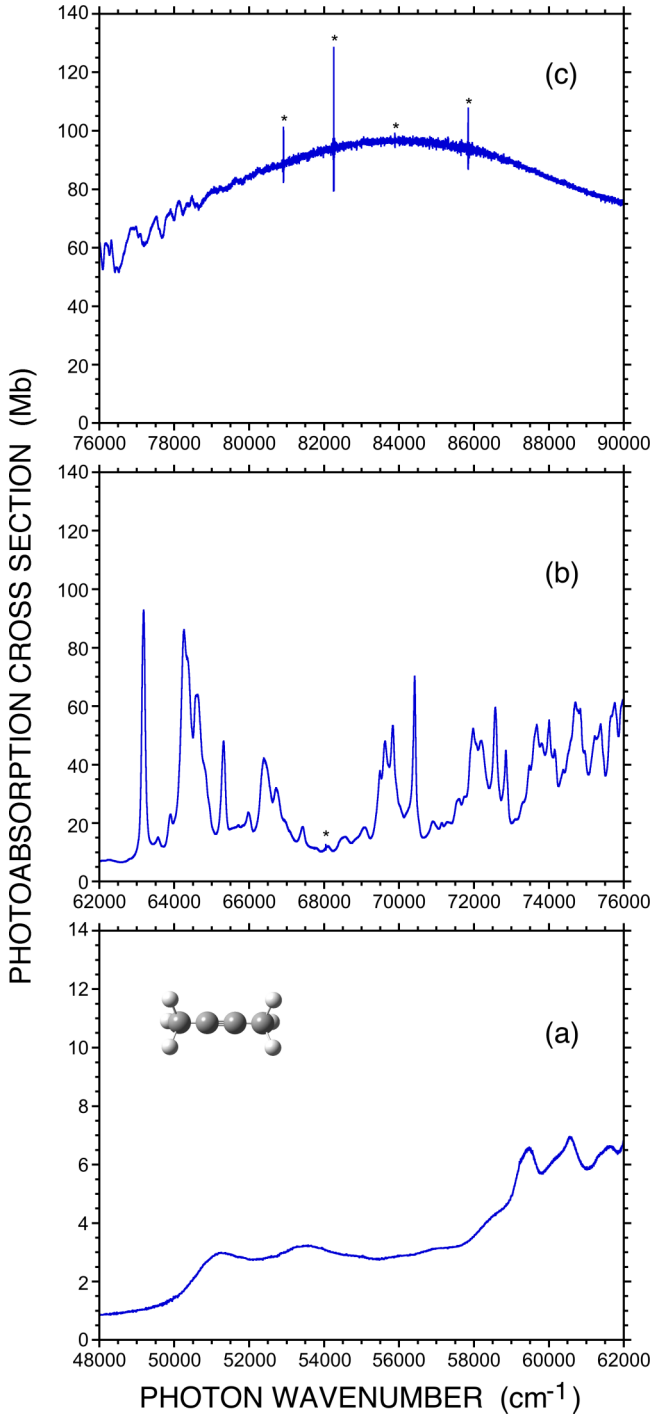

FIG. 7. The room-temperature absolute photoabsorption cross section of 2-butyne. Note that the scale of the y-axis in part (a) is a factor of ten smaller than in parts (b) and (c). The sharp lines marked by asterisks correspond to absorption transitions in atomic impurities (see text in Sec. II).

chemical calculations and their assignments of the $n = 3$ bands. The structure associated with vibrationally excited bands with $n^* = 3$ (i.e., between 65 000 cm^{-1} and 68 000 cm^{-1}) has also been blocked out to simplify the pattern recognition. The present spectrum shown in Figure 10 is somewhat better resolved than the earlier spectrum. As a result, at each value of n, some of the blended features in the earlier spectrum are resolved into two or more features. Palmer and Walker[8] assigned the intense feature at ~72 500 cm^{-1} as an overlap

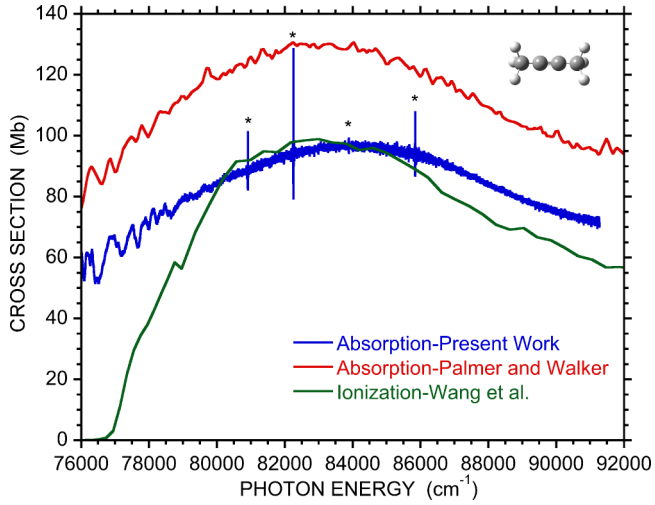

FIG. 8. An expanded portion of the room-temperature, absolute photoabsorption cross section of 2-butyne across the shape resonance, with an estimated uncertainty of ±10%. The photoabsorption data of Palmer and Walker[8] and the present experiment are shown. Also shown is the photoionization cross section reported by Wang *et al.*,[12] which has a reported uncertainty of ±20%. The observation that the absorption and ionization data are nearly parallel across the peak of the shape resonance suggests that the ionization quantum yield for the resonant component is nearly unity. The true photoionization cross section must be below or equal to the photoabsorption cross section, and this requirement is met when the uncertainties of the measurements are taken into account. The sharp lines marked by asterisks correspond to absorption transitions in atomic impurities (see text in Sec. II).

of two bands. The first corresponds to the $5d_{xy,x^2-y^2}$, $\nu_2' = 0$ band, and the second corresponds to the 4d, $\nu_2' = 1$ band; the latter assignment was made because the spacing between this feature and the 4d, $\nu_2' = 0$ band is very close to the ν_2^+ frequency. While this assignment is certainly plausible, three factors suggest that another explanation may be in order. First, the intensity of the 72 500 cm^{-1} feature is quite large for a $\nu_2' = 1$ band; indeed, because it is broad, the integrated intensity of this feature is nearly equal to that of the 4d, $\nu_2' = 0$ band. Second, the n^* value (with respect to the vibrationless ground state of the ion) for the $5d_{xy,x^2-y^2}$, $\nu_2' = 0$ assignment

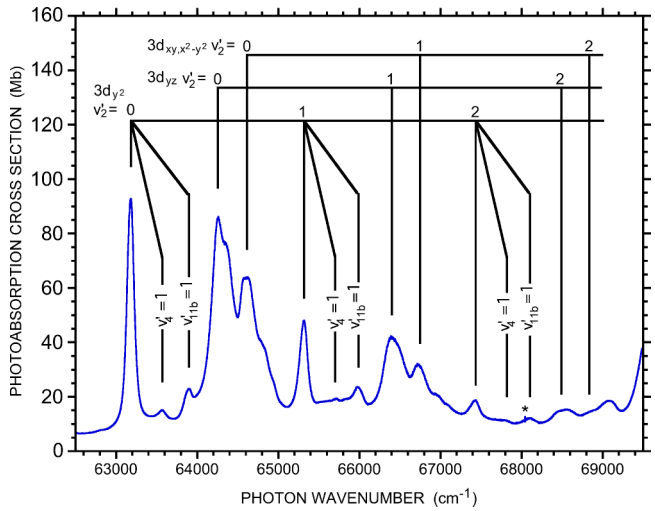

FIG. 9. An expanded portion of the room-temperature absolute photoabsorption cross section of 2-butyne in the region containing the transitions to states with $n^* = 3$. The assignments are from the work of Palmer and Walker.[8]

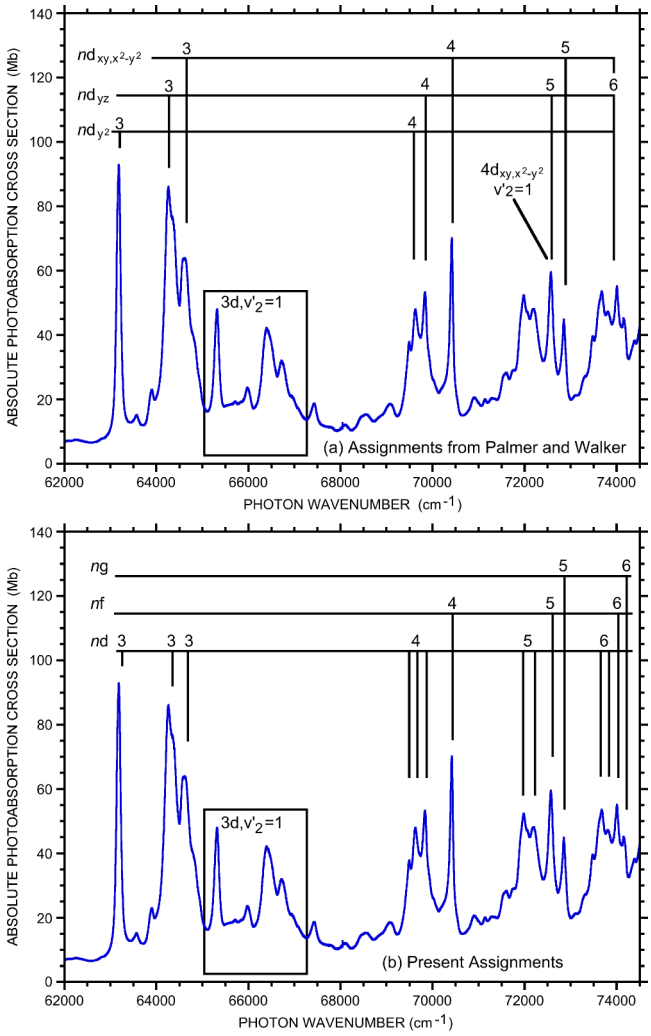

FIG. 10. An expanded portion of the room-temperature absolute photoabsorption cross section of 2-butyne in the region containing the transitions to states with $n^* = 3$–6. Both frames show the same experimental data from the present work, but with different assignments for the observed features. (a) The assignments of Palmer and Walker,[8] based on a somewhat lower resolution photoabsorption spectrum. (b) The present assignments suggesting the observation of transitions to Rydberg states with $l = 4$ and 5.

is $n^* = 4.9092$, i.e., $\delta = 0.0918$, whereas the corresponding value for the $4d_{xy,x^2-y^2}$, $v_2' = 0$ band is $n^* = 4.0459$, i.e., $\delta = -0.0459$. This shift is substantial for consecutive members of a Rydberg series and casts some doubt on the assignment. Third, and perhaps most important, the pattern of features at $n = 5$ is very similar to the pattern of features at $n = 6$, where no vibrational interlopers are expected. Figure 10(b) shows the same spectrum as Figure 10(a), but with a different set of assignments.[37] These assignments result from associating the new features at $n = 4$ and 5 with the first members of nf and ng Rydberg series, respectively. The introduction of these states at $n = 4$ and 5 perturbs the positions of the existing, lower-l states at these n values. This assignment is also consistent with the similar patterns at $n^* = 5$ and 6, suggesting that the four sharp features at each n represent the origin bands of successive members of four different Rydberg series. As discussed below, such an interpretation could also provide an explanation for the very different pattern of features at $n = 3$ and 4.

Although Palmer and Walker[8] assigned the features observed near $n^* = 4$ to the same three series they identified near $n^* = 3$, the actual pattern of levels is quite different. At $n^* = 3$, there is an intense, sharp, isolated band, followed by at least two strong overlapped bands at slightly higher energy. All of these features have values of $n^* < 3$. In contrast, at $n^* = 4$, there are at least three overlapped bands with $n^* < 4$, as well as a single isolated and intense band with n^* just greater than 4. Although the peaks are less resolved at higher n, the pattern at $n^* = 5$ is changed once again, with the addition of one more intense feature. At $n^* = 6$, however, the pattern is very similar to that at $n^* = 5$, albeit somewhat less resolved. The features at higher n^* are also consistent with the envelopes of the $n^* = 5$ and 6 features.

One explanation for the observation of new features at $n = 4$ and 5 is that new Rydberg series, specifically the nf, $l = 3$ and ng, $l = 4$ series, become accessible at these two values of n, respectively. In general, it is often assumed that the higher l Rydberg states will be nonpenetrating, with relatively small oscillator strength from the ground state of the molecule. It appears that for this reason, Palmer and Walker[8] did not perform calculations for the nf or higher l Rydberg states of 2-butyne. The single center expansion of the HOMO gives 74.1% $l = 1$; 0.1% $l = 2$; 14.9% $l = 3$; 0.4% $l = 4$; and 6.8% $l = 5$, with the remaining 3.7% distributed amongst higher partial waves. Thus, the HOMO of 2-butyne has significant high-l character suggesting that transitions to high-l Rydberg states may be more important than previously thought. Furthermore, the very intense $l = 4$, $g\pi_g^*$ shape resonance peaks just above the ionization threshold.[9] The width of this resonance is sufficient that its influence likely extends well below threshold, leading to enhanced intensity in the ng Rydberg series. If this interpretation is correct, the new feature observed at $n^* = 4$ would correspond to the $n = 4$ member of an f Rydberg series, and the new feature observed at $n^* = 5$ would correspond to the $n = 5$ member of a g Rydberg series. To the extent that these series perturb the lower l Rydberg series, they are expected to result in shifts of the corresponding quantum defects at $n = 4$ and 5. Such behavior is not unprecedented. For example, the interaction between the ndσ and $(n + 1)$sσ Rydberg states of NO leads to a significant shift in the sσ quantum defect between $n = 2$, where there is no corresponding dσ state, and $n = 3$, where the dσ state first appears.[38,39] What makes this observation somewhat surprising in the present context is that the perturbations occur between states that are normally considered non-penetrating. In Section III C, we use theoretical calculations and concepts from quantum defect theory to generate support for this interpretation.

At higher principal quantum number, the structure in the 2-butyne spectrum becomes more erratic, as seen in Figure 11. For the lowest n values shown in Figure 11 (i.e., $n = 7, 8$), some of the structure observed at $n < 7$ remains, but the features are blended and become unresolved at $n > 9$. No interlopers based on electronically excited ion states appear to be present in the energy region of the figure. (The first electronic excited state threshold for the ion lies at ~115 300 cm^{-1},[35] and Rydberg states converging to this limit are only expected at higher energy.) Thus, the irregularity in the spectrum is most likely due to interference among the Rydberg series converging to

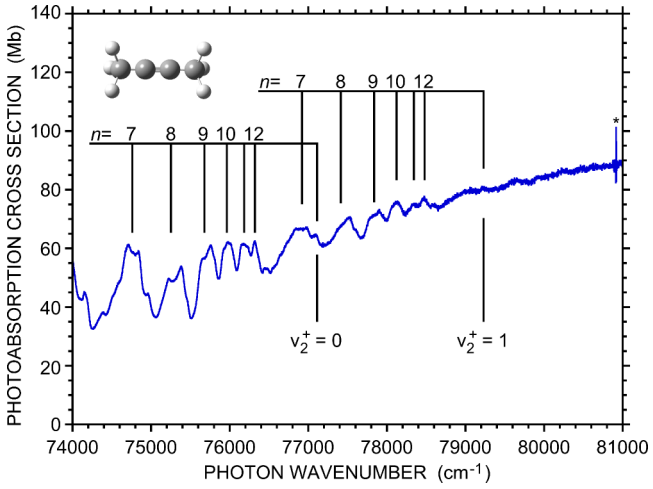

FIG. 11. The room-temperature photoabsorption spectrum of 2-butyne near the first ionization threshold. Tentative assignments of the Rydberg series converging to the vibrationless ground state of the cation are indicated. The $v_2^+ = 0$ and 1 thresholds at 77 120 cm^{-1} and 79 233 cm^{-1}, respectively, are also indicated.

vibrationally excited levels of the ground state cation. The $v_2^+ = 0$ and 1 ionization thresholds are indicated in the figure. As observed previously in the photoabsorption spectrum of propyne,[9] the appearance of the spectrum strongly suggests that the dominant Rydberg series in this region converge to these thresholds. As in the case of propyne,[9] there is also a strong similarity of the structure converging to the $v_2^+ = 0$ and 1 thresholds, suggesting very regular perturbations between series converging to successive thresholds (i.e., between $v_2^+ = 0$ and 1 series, and between $v_2^+ = 1$ and 2 series).

C. Theoretical considerations for 2-butyne

We would like to assess the potential role of high-l Rydberg states ($l \geq 3$) in the photoabsorption spectrum of 2-butyne. This assessment requires two principal tasks. First, we must assess how strong the series with $l \geq 3$ are likely to be in transitions from the ground state. Second, we must try to estimate the energy positions of these states and assess the extent to which these states perturb the positions of the other Rydberg states relative to their positions at lower n, i.e., where the high-l states no longer exist.

We first consider the transition probabilities to higher l states. As noted above, there have been no direct calculations of nf, ng, or higher l Rydberg states or of the transitions to them from the ground state of 2-butyne. In general, such calculations are difficult for larger molecules due to the increasing number of states at $n = 4$, 5, and higher. Furthermore, in this region, the typical errors in the predicted energy levels relative to experiment are on the order of 0.2–0.4 eV. Because the spacing between the $n = 4$ and 5 manifolds is ~0.3 eV, assignments based on the predicted energies are difficult, even if all of the relevant states are included in the calculation. While models based solely on long-range interactions for purely non-penetrating states have been quite successful,[40–42] we expect the f and g series of interest in 2-butyne to have sufficient penetrating character to require a more complete treatment. In the absence of traditional quantum chemical calculations, we have performed calculations of the photoabsorption cross section just above the ionization threshold. These calculations allow the break down of the cross section into contributions from partial waves with different values of l. Using the principle of continuity of oscillator strength through an ionization threshold,[24,25] these calculations shed light on the expected relative strengths of Rydberg series below the threshold and thus can aid or support the assignment of the spectrum.

In the present calculation, the continuum is described as a sum over a large number of partial waves, with l ranging from 0 to 10. The photoabsorption calculations were performed by using the ePolyScat codes[43,44] within the frozen-core Hartree-Fock (FCHF) approximation.[45] In this approach, the continuum electron wave function is calculated on a numerical grid based on a single-center expansion, where partial waves up to $l_{max} = 60$ were included for convergence in the short-range region around the nuclei. The bound orbitals of the target were obtained from restricted Hartree-Fock wave functions computed using the Gaussian code[28] and an augmented correlation consistent polarized valence triple-zeta (aug-cc-pVTZ) one-electron basis set.[46,47] The calculations were performed in the fixed-nuclei approximation at a geometry obtained from an optimization using second order Møller-Plesset perturbation theory and the same aug-cc-pVTZ basis set. The transition moments were calculated in both the length and velocity gauges, as well as the length/velocity mixed gauge.

The transition moments from the 2-butyne ground state to the continua with $l = 0$–6 and for a photon energy of 78 236 cm^{-1} (970 cm^{-1} above the calculated ionization threshold) are shown in Table III. Figure 12 shows the continuum partial photoionization cross sections as a function of photon energy and broken down by l. While we are interested in the transition moments to the bound states near $n = 4$ and 5, i.e., near 70 170 cm^{-1}, the principle of continuity of oscillator strength[24,25] requires that the transition moments just above threshold will merge smoothly into those for the Rydberg states just below threshold. Thus, while some energy dependence is certainly expected, continua with significant oscillator strength just above threshold should be connected with Rydberg states with significant intensity below threshold. Of course, just above threshold, the transition moment to the $l = 4$ gπ continuum is increasing rapidly due to the shape resonance of the same symmetry.[9] As a result, at lower energy, the intensity of the corresponding Rydberg series may be reduced considerably. Nevertheless, Figure 12 shows that, even at energies well below the peak of the resonance, the transition moment to the $l = 4$ gπ continuum is still quite strong. These results suggest that gπ series might still have significant intensity even at $n = 5$.

Based on Table III, the two strongest series are expected to be what are nominally fδ and gπ Rydberg series, providing significant support for the assignments proposed here. The next most intense series are expected to be more traditional dδ and sσ series, followed by a variety of significantly weaker nd and ng series. The latter series are probably significantly weaker at the energy of the $n = 5$ Rydberg states.

TABLE III. Partial photoionization cross sections of 2-butyne for different partial waves.[a]

l	$\|m\|$	σ_{length} (Mb)	Fraction (length)	$\sigma_{velocity}$ (Mb)	Fraction (velocity)	σ_{mixed} (Mb)	Fraction (mixed)
0	0	4.3160	0.079	4.6017	0.132	4.4533	0.103
1	0	0.0000	0.000	0.0000	0.000	0.0000	0.000
1	1	0.0214	0.000	0.0135	0.000	0.0168	0.000
2	0	1.2604	0.023	1.1340	0.032	1.1837	0.027
2	1	1.8655	0.034	1.0409	0.030	1.3930	0.032
2	2	8.3717	0.154	5.8483	0.167	6.9036	0.160
3	0	0.0000	0.000	0.0000	0.000	0.0000	0.000
3	1	0.2328	0.004	0.1675	0.005	0.1972	0.005
3	2	16.5151	0.303	9.1111	0.261	12.2654	0.284
3	3	0.1328	0.002	0.1124	0.003	0.1222	0.003
4	0	1.6456	0.030	1.3907	0.040	1.5128	0.035
4	1	16.8330	0.309	9.5186	0.272	12.6577	0.293
4	2	3.1274	0.057	1.9611	0.056	2.4718	0.057
4	3	0.0496	0.001	0.0392	0.001	0.0415	0.001
4	4	0.0013	0.000	0.0007	0.000	0.0010	0.000
5	0	0.0000	0.000	0.0000	0.000	0.0000	0.000
5	1	0.0000	0.000	0.0000	0.000	0.0000	0.000
5	2	0.0438	0.001	0.0246	0.001	0.0328	0.001
5	3	0.0024	0.000	0.0018	0.000	0.0021	0.000
5	4	0.0003	0.000	0.0001	0.000	0.0001	0.000
5	5	0.0000	0.000	0.0000	0.000	0.0001	0.000
6	0	0.0002	0.000	0.0002	0.000	0.0002	0.000
6	1	0.0019	0.000	0.0011	0.000	0.0014	0.000
6	2	0.0008	0.000	0.0005	0.000	0.0006	0.000
6	3	0.0000	0.000	0.0000	0.000	0.0000	0.000
6	4	0.0000	0.000	0.0000	0.000	0.0000	0.000
6	5	0.0000	0.000	0.0000	0.000	0.0000	0.000
6	6	0.0000	0.000	0.0000	0.000	0.0000	0.000
Total		54.422		34.968		43.257	

[a]The partial cross sections (in units of Mb, i.e., 10^{-18} cm^2) were calculated as described in Ref. 7 at a photon energy of 78 236 cm^{-1}, which lies 970 cm^{-1} above the calculated ionization threshold (77 266 cm^{-1}). The transition moments were calculated using the length-, velocity-, and mixed-gauge forms of the transition dipole matrix element. The differences between the forms give a rough indication of the expected accuracy of the calculations. The total cross sections were calculated including partial waves up to $l = 10$, but the contribution of all $l > 6$ is quite small. The calculations yield fixed-nuclei photoionization cross sections, but because the ionization yield is implicitly 1.0, the results are best compared to the photoabsorption cross section.

Perhaps the most surprising thing about Table III and Figure 12 is the magnitude of the $l = 3$ cross section (in particular, $l = 3$, $|m| = 2$). As discussed above, the single-center expansion of the ground state HOMO is almost completely made up of odd-l contributions. Based on the $\Delta l = \pm 1$ selection rule, this situation suggests that transitions to odd-l continua will be weak. The calculations were performed in a D_3 geometry, where even and odd l are mixed. Interestingly, a calculation in a D_{3d} geometry, in which this mixing cannot occur and only even l are allowed, yields approximately the same total cross section as the calculation in the D_3 geometry. This observation suggests that all of the intensity in the $l = 3$ partial cross section is "borrowed" from the $l = 2$ and 4 partial cross sections.

Finally, we must assess the extent to which the nf and ng Rydberg states are expected to perturb the positions of the other Rydberg states observed in the spectrum. In Table II, the effective principal quantum number for the three strong features assigned previously to 3d Rydberg states is $n^* = 2.8056$, 2.9205, and 2.9573. The 3d and 4s states are likely mixed, so we label these states accordingly as 3d/4s. With our proposed assignments, the corresponding s/d features at $n = 4$ have $n^* = 3.7922$, 3.8262, and 3.8806; the new feature at $n = 4$, which is assigned to a 4f state, has $n^* = 4.0459$. Thus, while the lowest 4d state is not significantly perturbed, the other two are pushed to somewhat lower n^* values than expected by the 4f state. If this interpretation is correct, the n^* value of the 4f state is likely somewhat higher than it would have been in the absence of d-f interactions. At $n = 5$, the corresponding 5d features (only two are resolved) have $n^* = 4.6209$ and 4.7199, and the 5f feature has $n^* = 4.9092$. The new feature, which has been assigned as a 5g state, has $n^* = 5.0709$. Thus, in this scheme, the introduction of the 5g state pushes the 5f state to lower energy than expected, which in turn pushes the 5d/6s states to still lower energy. We note that these perturbations, which involve interactions between even-l and odd-l Rydberg series, are the same interactions responsible for the enhancement of the $l = 3$ partial photoionization cross

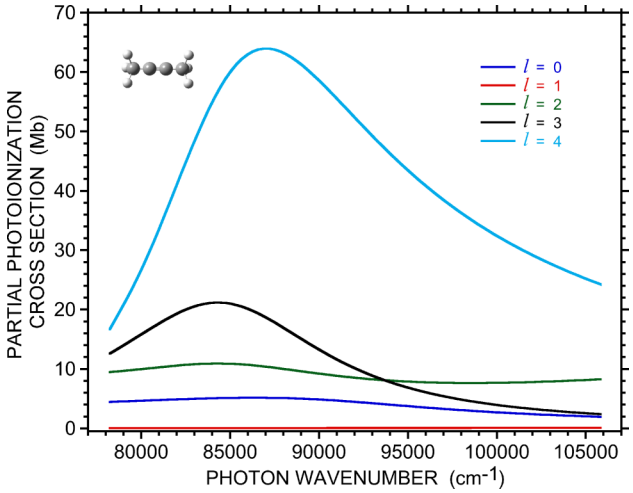

FIG. 12. The calculated partial photoionization cross sections of 2-butyne as a function of l and photon energy.

section discussed above. Thus, some qualitative support exists for the present assignment of the 2-butyne spectrum. At higher n, the spectrum appears to become more regular, although the individual series are considerably less resolved.

In the absence of such an assignment, the relatively strong energy dependence of the n^* values between $n = 3$ and 5 would be much harder to rationalize. Of course, it is possible that interactions between states converging to different vibrational thresholds could be responsible for these perturbations. However, as discussed above, the intensities of the series converging to vibrationally excited states of the ground electronic state of the ion are less than half the intensity of those of the origin bands. Furthermore, the interactions between series with different vibrational quantum numbers tend to be relatively weak.[48] Such interactions are also responsible for vibrational autoionization,[49–51] and the strongest generally have $\Delta v_i = 1$. The widths of the vibrationally autoionizing levels in Figure 11 are not particularly large, so it seems less likely that vibrational perturbations are responsible for the observations. Another possibility is that Rydberg-valence interactions are responsible for the perturbations and energy shifts, but so far there is no self-consistent explanation for the observations from that perspective.

A quantitative determination of the expected perturbations between nd, nf, and ng Rydberg states in 2-butyne would be highly desirable. As discussed above, detailed quantum chemical calculations on these states are challenging and have yet to be performed. Alternatively, it may be possible to use information from the partial-wave analysis of the photoionization cross sections to characterize the interactions between partial waves with different l and thus provide insight into the d-f-g interactions. Such an analysis would make use of the connection between the scattering phase shifts for the continuum and the quantum defects for the bound states. We are currently exploring this possibility.

IV. CONCLUSION

New room-temperature, absolute photoabsorption cross sections were recorded for 1- and 2-butyne by using the vacuum ultraviolet Fourier-Transform spectrometer at the SOLEIL Synchrotron. The results are in good agreement with previous measurements for these two molecules, but the higher resolution of the present measurements reveals additional structure, particularly for 2-butyne. Analysis of the 1-butyne spectrum only leads to modest additions to the previous work,[2] corresponding to the observation of additional vibrational structure in the low-energy bands. Examination of the 2-butyne spectrum suggests a reassignment of some of the features at effective principal quantum number $n = 4$ and 5. We argue that the nf and ng Rydberg states in the photoabsorption spectrum of 2-butyne will be considerably more intense than normally expected. Because quantitative quantum chemical calculations of the photoabsorption spectrum in this energy region are difficult, we have developed other approaches to interpret and rationalize the results. In particular, the present arguments are based both on the nature of the HOMO in the ground state neutral and on theoretical calculations of the photoabsorption spectrum above the ionization threshold. The latter calculations are valuable because they provide a direct indication of the relative importance of partial waves (and thus Rydberg series) with different values of l. Although this approach provides the basis for a self-consistent analysis of the observed 2-butyne spectrum, confirmation must await a more detailed and comprehensive theoretical analysis. We suggest that an analysis of the phase shifts in theoretical partial cross sections for photoionization may provide the required insight for a more quantitative assignment of the spectrum. Nevertheless, as in our earlier work on propyne, we believe the present results argue strongly for the importance of high-l states ($l \geq 3$) in the photoabsorption spectra of larger n-alkynes.

ACKNOWLEDGMENTS

D.M.P.H. was supported by the Science and Technology Facilities Council, UK. This material is based on work supported by the U.S. Department of Energy, Office of Science, Office of Basic Energy Sciences, Division of Chemical Sciences, Geosciences, and Biosciences, respectively, under Contract Nos. DE-AC02-06CH11357 (for H.X. and S.T.P.) and DE-SC0012198 (for R.R.L.). R.R.L. also acknowledges the support of the Robert A. Welch Foundation under Grant No. A-1020. This work was supported by the Texas A&M University Supercomputing Facility. The work was performed on the DESIRS Beamline at SOLEIL under Proposal No. 20120675. We are grateful to Laurent Nahon of the DESIRS Beamline for his help and guidance and to the whole staff of SOLEIL for running the facility.

[1]K. Watanabe and T. Namioka, J. Chem. Phys. **24**, 915 (1956).
[2]T. Nakayama and K. Watanabe, J. Chem. Phys. **40**, 558–561 (1964).
[3]J. C. Person and P. P. Nicole, J. Chem. Phys. **53**, 1767–1774 (1970).
[4]G. H. Ho, M. S. Lin, Y. L. Wang, and T. W. Chang, J. Chem. Phys. **109**, 5868–5879 (1998).
[5]M. H. Palmer, C. C. Ballard, and I. C. Walker, Chem. Phys. **249**, 129–144 (1999).
[6]J. C. Shieh, J. L. Chang, J. C. Wu, R. Li, A. M. Mebel, N. C. Handy, and Y. T. Chen, J. Chem. Phys. **112**, 7384–7393 (2000).
[7]U. Jacovella, D. M. P. Holland, S. Boyé-Péronne, D. Joyeux, L. E. Archer, N. de Oliveira, L. Nahon, R. R. Lucchese, H. Xu, and S. T. Pratt, J. Chem. Phys. **141**, 114303 (2014).
[8]M. H. Palmer and I. C. Walker, Chem. Phys. **340**, 158–170 (2007).

[9]H. Xu, U. Jacovella, B. Ruscic, S. T. Pratt, and R. R. Lucchese, J. Chem. Phys. **136**, 154303 (2012).
[10]S. Hamai and F. Hirayama, J. Chem. Phys. **71**, 2934–2939 (1979).
[11]T. A. Cool, K. Nakajima, T. A. Moustefaoui, F. Qi, A. McIlroy, P. R. Westmoreland, M. E. Law, L. Poisson, D. S. Peterka, and M. Ahmed, J. Chem. Phys. **119**, 8356–8365 (2003).
[12]J. Wang, B. Yang, T. A. Cool, N. Hansen, and T. Kasper, Int. J. Mass Spectrom. **269**, 210–220 (2008).
[13]B. Yang, J. Wang, T. A. Cool, N. Hansen, S. Skeen, and D. L. Osborn, Int. J. Mass Spectrom. **247**, 118–128 (2012).
[14]C. A. Taatjes, N. Hansen, A. McIlroy, J. A. Miller, J. P. Senosiain, S. J. Klippenstein, F. Qi, L. S. Sheng, Y. W. Zhang, T. A. Cool, J. Wang, P. R. Westmoreland, M. E. Law, T. Kasper, and K. Kohse-Hoinghaus, Science **308**, 1887 (2005).
[15]J. Berkowitz, *Photoabsorption, Photoionization, and Photoelectron Spectroscopy* (Academic, New York, 1979).
[16]J. Berkowitz, *Atomic and Molecular Absorption* (Academic, San Diego, 2002).
[17]A. Tramer, Ch. Jungen, and F. Lahmani, *Energy Dissipation in Molecular Systems* (Springer, Heidelberg, 2010).
[18]H. Koizumi, J. Chem. Phys. **95**, 5846–5853 (1991).
[19]M. Bobeldijk, W. J. van der Zande, and P. G. Kistemaker, Chem. Phys. **179**, 125–130 (1994).
[20]H. Xu and S. T. Pratt, J. Phys. Chem. A **117**, 9331–9342 (2013).
[21]M. B. Robin, in *Higher Excited States of Polyatomic Molecules* (Academic, New York, 1974), Vol. 1.
[22]M. B. Robin, in *Higher Excited States of Polyatomic Molecules* (Academic, New York, 1975), Vol. 2.
[23]M. B. Robin, in *Higher Excited States of Polyatomic Molecules* (Academic, New York, 1985), Vol. 3.
[24]A. C. Allison and A. Dalgarno, J. Chem. Phys. **55**, 4342–4344 (1971).
[25]A. L. Smith, J. Chem. Phys. **55**, 4344–4350 (1971).
[26]T. A. Cool, J. Wang, K. Nakajima, C. A. Taatjes, and A. McIlroy, Int. J. Mass Spectrom. **247**, 18–27 (2005).
[27]W. L. Jorgensen and L. Salem, *The Organic Chemist's Book of Orbitals* (Academic, New York, 1973).
[28]M. J. Frisch, G. W. Trucks, H. B. Schlegel, G. E. Scuseria, M. A. Robb, J. R. Cheeseman, G. Scalmani, V. Barone, B. Mennucci, G. A. Petersson, H. Nakatsuji, M. Caricato, X. Li, H. P. Hratchian, A. F. Izmaylov, J. Bloino, G. Zheng, J. L. Sonnenberg, M. Hada, M. Ehara, K. Toyota, R. Fukuda, J. Hasegawa, M. Ishida, T. Nakajima, Y. Honda, O. Kitao, H. Nakai, T. Vreven, J. A. Montgomery, Jr., J. E. Peralta, F. Ogliaro, M. Bearpark, J. J. Heyd, E. Brothers, K. N. Kudin, V. N. Staroverov, R. Kobayashi, J. Normand, K. Raghavachari, A. Rendell, J. C. Burant, S. S. Iyengar, J. Tomasi, M. Cossi, N. Rega, J. M. Millam, M. Klene, J. E. Knox, J. B. Cross, V. Bakken, C. Adamo, J. Jaramillo, R. Gomperts, R. E. Stratmann, O. Yazyev, A. J. Austin, R. Cammi, C. Pomelli, J. W. Ochterski, R. L. Martin, K. Morokuma, V. G. Zakrzewski, G. A. Voth, P. Salvador, J. J. Dannenberg, S. Dapprich, A. D. Daniels, Ö. Farkas, J. B. Foresman, J. V. Ortiz, J. Cioslowski, and D. J. Fox, GAUSSIAN 09, Revision D.01, Gaussian, Inc., Wallingford, CT, 2009.
[29]N. de Oliveira, D. Joyeux, D. Phalippou, J. C. Rodier, F. Polack, M. Vervloet, and L. Nahon, Rev. Sci. Instrum. **80**, 043101 (2009).
[30]N. de Oliveira, M. Roudjane, D. Joyeux, D. Phalippou, J. C. Rodier, and L. Nahon, Nat. Photonics **5**, 149–153 (2011).
[31]A detailed discussion of potential sources of error in cross sections determined with the FTS will be presented in a forthcoming publication by N. de Oliveira, D. Joyeux, L. E. Archer, J. F. Gil, M. Roudjane, K. Ito, and L. Nahon.
[32]See http://webbook.nist.gov for "NIST Chemistry WebBook."
[33]P. Carlier, J. E. Dubois, P. Masclet, and G. Mouvier, J. Electron Spectrosc. Relat. Phenom. **7**, 55–67 (1975).
[34]C. di Lauro, P. R. Bunker, J. W. C. Johns, and A. R. W. McKellar, J. Mol. Spectrosc. **184**, 177–185 (1997).
[35]G. Bieri, F. Burger, E. Heilbronner, and J. P. Maier, Helv. Chim. Acta **60**, 2213–2233 (1977).
[36]U. Jacovella, B. Gans, and F. Merkt, "Internal rotation, spin–orbit coupling, and low-frequency vibrations in the $\tilde{X}^+\,^2E$ ground state of CH_3–CC–CH_3^+ and CD_3–CC–CD_3^+," Mol. Phys. (published online).
[37]See supplementary material at http://dx.doi.org/10.1063/1.4926541 for a plot of the data of Figure 10 against n^* rather than energy.
[38]Ch. Jungen, J. Chem. Phys. **53**, 4168–4182 (1970).
[39]M. R. Hermann, C. W. Bauschlicher, Jr., W. M. Huo, S. R. Langhoff, and P. W. Langhoff, Chem. Phys. **109**, 1–23 (1986).
[40]Ch. Jungen and E. Miescher, Can. J. Phys. **47**, 1769–1787 (1969).
[41]E. E. Eyler and F. M. Pipkin, Phys. Rev. A **27**, 2462–2478 (1983).
[42]G. Herzberg and Ch. Jungen, J. Chem. Phys. **84**, 1181–1192 (1986).
[43]F. A. Gianturco, R. R. Lucchese, and N. Sanna, J. Chem. Phys. **100**, 6464–6471 (1994).
[44]A. P. P. Natalense and R. R. Lucchese, J. Chem. Phys. **111**, 5344–5348 (1999).
[45]R. R. Lucchese, G. Raseev, and V. McKoy, Phys. Rev. A **25**, 2572–2587 (1982).
[46]T. H. Dunning, Jr., J. Chem. Phys. **90**, 1007–1023 (1989).
[47]R. A. Kendall, T. H. Dunning, Jr., and R. Harrison, J. Chem. Phys. **96**, 6796–6806 (1992).
[48]H. Lefebvre-Brion and R. W. Field, *The Spectra and Dynamics of Diatomic Molecules* (Elsevier, Amsterdam, 2004).
[49]R. S. Berry, J. Chem. Phys. **45**, 1228–1245 (1966).
[50]G. Herzberg and Ch. Jungen, J. Mol. Spectrosc. **41**, 425–486 (1972).
[51]Ch. Jungen and S. T. Pratt, J. Chem. Phys. **106**, 9529–9538 (1997).